The human *Tp53 Arg72Pro* polymorphism explains different functional prognosis in stroke

Jose C. Gomez-Sanchez,[1] Maria Delgado-Esteban,[2] Irene Rodriguez-Hernandez,[3] Tomas Sobrino,[4] Natalia Perez de la Ossa,[6] Silvia Reverte,[6] Juan P. Bolaños,[7] Rogelio Gonzalez-Sarmiento,[3] Jose Castillo,[4,5] and Angeles Almeida[2,7]

[1]Department of Neurology, University Hospital of Salamanca, 37007 Salamanca, Spain
[2]Research Unit, University Hospital of Salamanca and Institute of Health Sciences of Castilla and Leon, 37007 Salamanca, Spain
[3]Department of Medicine and Center for Cancer Research, University of Salamanca and Consejo Superior de Investigaciones Científicas, 37007 Salamanca, Spain
[4]Clinical Neuroscience Research Laboratory and [5]Department of Neurology, University Hospital and University of Santiago de Compostela, 15706 Santiago de Compostela, Spain
[6]Stroke Unit, Department of Neurosciences, University Hospital Germans Trias i Pujol, Universitat Autònoma de Barcelona, 08916 Barcelona, Spain
[7]Department of Biochemistry and Molecular Biology, University of Salamanca, 37007 Salamanca, Spain

The functional outcome after stroke is unpredictable; it is not accurately predicted by clinical pictures upon hospital admission. The presence of apoptotic neurons in the ischemic penumbra and perihematoma area may account for poor prognosis, but whether the highly variable stroke outcome reflects differences in genetic susceptibility to apoptosis is elusive. The p53 tumor suppressor protein, an important transcriptional regulator of apoptosis, naturally occurs in humans in two variants with single nucleotide polymorphisms resulting in *Arg* or *Pro* at residue 72. We show that poor functional outcome after either ischemic or hemorrhagic stroke was linked to the *Arg/Arg* genotype. This genotype was also associated with early neurological deterioration in ischemic stroke and with increased residual cavity volume in intracerebral hemorrhage. In primary cultured neurons, Arg^{72}-p53, but not Pro^{72}-p53, interacted directly with mitochondrial Bcl-xL and activated the intrinsic apoptotic pathway, increasing vulnerability to ischemia-induced apoptotic cell death. These results suggest that the *Tp53 Arg/Arg* genotype governs neuronal vulnerability to apoptosis and can be considered as a genetic marker predicting poor functional outcome after stroke.

CORRESPONDENCE
Angeles Almeida:
aaparra@usal.es

Abbreviations used: $\Delta\psi_m$, mitochondrial membrane potential; BAC, bacterial artificial chromosome; CI, confidence interval; END, early neurological deterioration; ICH, intracerebral hemorrhage; mRS, modified Rankin Scale; NIHSS, National Institutes of Health Stroke Scale; OR, odds ratio; PFT-α, pifithrin α; SNP, single nucleotide polymorphism.

Stroke is the leading neurological cause of death and severe long-term disability in developed countries (Rosamond et al., 2008), although functional outcome after stroke is still largely unpredictable (Baird et al., 2001; Weimar et al., 2002; Muir et al., 2006). Patients initially showing a similar clinical picture can improve dramatically or worsen during the first days after stroke (Castillo, 1999; Baird, 2007). The presence of apoptotic neurons in the ischemic penumbra (Sairanen et al., 2006) and perihematoma area (Qureshi et al., 2003) may account for the impaired functional recovery of patients (Broughton et al., 2009) after ischemic stroke and intracerebral hemorrhage (ICH), respectively. Thus, the highly variable prediction of functional outcome after stroke could be the effect of different genetic backgrounds to apoptosis.

Tp53 encodes the p53 transcription factor, a tumor suppressor protein that mediates apoptosis in eukaryotic cells. Several polymorphisms have been identified within the *Tp53* gene, both in noncoding (introns) and coding (exons) regions (Olivier et al., 2002; Pietsch et al., 2006). The best studied human *Tp53* polymorphisms include the codon 72 (exon 4) single nucleotide polymorphism (SNP), which

J.C. Gomez-Sanchez, M. Delgado-Esteban, and I. Rodriguez-Hernandez contributed equally to this paper.

The Rockefeller University Press $30.00
J. Exp. Med. Vol. 208 No. 3 429-437
www.jem.org/cgi/doi/10.1084/jem.20101523

The Journal of Experimental Medicine

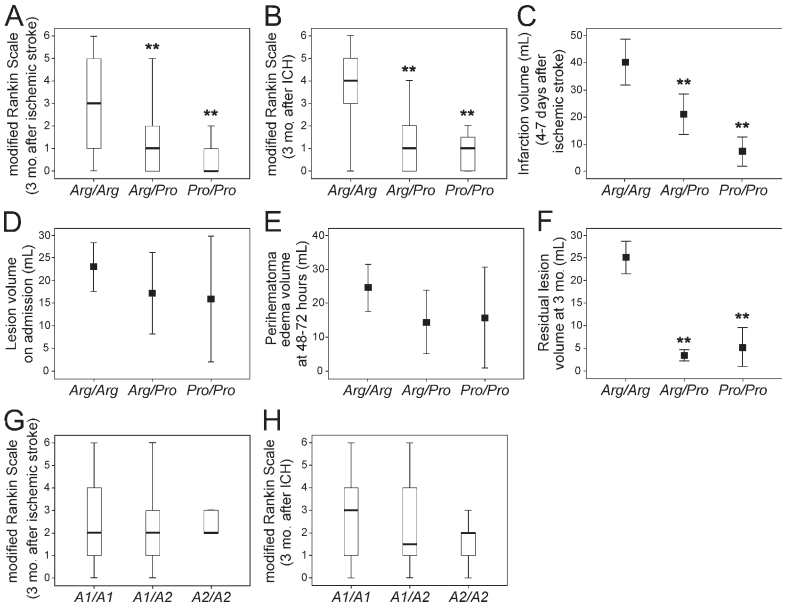

Figure 1. *Tp53* codon 72 polymorphism (*Arg72Pro*) determines functional outcome after ischemic stroke or ICH. Patients were admitted at the University Hospital of Santiago de Compostela (Galicia, Spain). The study included 408 (*Arg/Arg*: 235; *Arg/Pro*: 147; *Pro/Pro*: 26) patients with ischemic stroke (A and C) and 128 (*Arg/Arg*: 67; *Arg/Pro*: 54; *Pro/Pro*: 7) patients with ICH (B and D–F). Scores of the mRS (A and B), infarct volume (C), initial lesion volume (D), perihematoma edema volume (E), and residual cavity volume (F) were measured in patients with indicated *Tp53* codon 72 genotypes. Ischemic stroke (G) and ICH (H) patients were also classified according to *Ins16bp polymorphic variants* (*A1/A1*, *A1/A2*, and *A2/A2* genotypes) and mRS scores were measured. Box plots show median values (horizontal line inside the box), quartiles (box boundaries), and the largest and smallest observed values (error bars). Points represent mean values and error bars indicate standard deviation. **, $P < 0.001$ compared with *Arg/Arg* genotype.

leads to arginine-proline substitution (*Arg72Pro*), and a 16-bp duplication in intron 3 (*Ins16bp*; Pietsch et al., 2006). In contrast to *Ins16bp* polymorphism, the *Arg72Pro* SNP occurs in a proline-rich domain involved in the proapoptotic function of p53 (Sakamuro et al., 1997; Pietsch et al., 2006). Thus, the Arg^{72} variant of p53 is a more potent inducer of apoptosis and inhibitor of oncogenic transformation than the Pro^{72} variant (Dumont et al., 2003; Bonafé et al., 2004; Zhu et al., 2010), and this determines cancer progression, the age of onset, and the survival of individuals harboring the *Arg72Pro* SNP (Pietsch et al., 2006; Whibley et al., 2009).

In this paper, we aimed to investigate, using two independent hospital-based prospective cohorts of patients, whether the *Tp53* polymorphism affecting the apoptotic function of p53 (*Arg72Pro*) explains the differential functional outcome of individuals after stroke. To gain further support for the conclusions, we also included in the study haplotype analysis of the *Ins16bp* polymorphism. Finally, the molecular mechanism of apoptotic death caused by the *Arg72Pro* SNP variants was also investigated in cortical neurons in primary culture.

RESULTS AND DISCUSSION

The *Tp53 Arg/Arg* genotype is associated with poor functional outcome after stroke

Using the modified Rankin Scale (mRS; Sulter et al., 1999) to evaluate the disability or dependence in daily living activities of stroke victims (see Table S1 for baseline characteristics of patients), we found a median mRS score of ∼3 in patients harboring the *Arg/Arg* genotype at 3 mo after ischemic stroke. This mRS score was significantly higher than those found in *Arg/Pro* or *Pro/Pro* patients (Fig. 1 A and Fig. S1 A). However, no significant differences were found between groups of patients heterozygous and homozygous for the *Pro* allele (Fig. 1 A and Fig. S1 A), suggesting that this allele likely exerts a dominant effect over *Arg* (Biros et al., 2002; Bonafé et al., 2004). In ICH patients, we found that the mRS score was also significantly higher in *Arg/Arg* patients than in those harboring the *Arg/Pro* or *Pro/Pro* genotypes; carriers of the *Pro* allele showed a similar mRS score in ICH (Fig. 1 B and Fig. S1 B), as was also observed in ischemic stroke (Fig. 1 A and Fig. S1 A). Moreover, the percentage of patients with poor functional outcome (mRS > 2; Sulter et al., 1999) at 3 mo after either ischemic stroke or ICH was significantly higher in patients harboring the *Arg/Arg* genotype than in those with *Arg/Pro* or *Pro/Pro* genotypes in both cohorts studied (Table I).

Table I. Functional outcome after stroke according to *Tp53 Arg72Pro* genotypes

Genotype	Ischemic stroke				ICH			
	Cohort 1 (P < 0.0001)		Cohort 2 (P = 0.020)		Cohort 1 (P < 0.0001)		Cohort 2 (P = 0.004)	
	Good prognosis	Poor prognosis	Good prognosis	Poor prognosis	Good prognosis	Poor prognosis	Good prognosis	Poor prognosis
Arg/Arg	104 (44.3)	131 (55.7)	35 (57.4)	26 (42.6)	13 (19.4)	54 (80.6)	8 (26.7)	22 (73.3)
Arg/Pro	117 (79.6)	30 (20.4)	27 (77.1)	8 (22.9)	49 (90.7)	5 (9.3)	12 (75.0)	4 (25.0)
Pro/Pro	26 (100)	0	7 (100)	0	7 (100)	0	2 (100)	0

Cohort 1: patients were admitted at the University Hospital of Santiago de Compostela (Galicia, Spain). Cohort 2: patients were admitted at the University Hospital of Germans Trias i Pujol (Catalonia, Spain). Functional outcome was evaluated at 3 mo using the mRS. An mRS score >2 was considered poor prognosis. Data are numbers (%). Data were compared among genotype groups using the χ^2 test.

Table II. Univariate analysis of variables according to prognosis in stroke patients

Variable	Ischemic stroke			ICH		
	Good prognosis *n* = 247	Poor prognosis *n* = 161	P value	Good prognosis *n* = 69	Poor prognosis *n* = 59	P-value
Age, years	70.1 (11.7)	78.8 (9.9)	<0.0001	69.3 (13.6)	76.4 (9.5)	0.009
Males, %	68.0	46.0	<0.0001	56.5	59.3	0.445
Hypertension, %	51.1	64.6	0.007	55.1	55.9	0.532
Diabetes, %	27.1	24.8	0.347	10.1	28.8	0.007
Smoking, %	17.4	8.1	0.005	10.1	11.9	0.487
Heavy alcohol intake, %	9.3	7.5	0.321	17.4	11.9	0.267
Hyperlipidemia, %	33.2	28.6	0.191			
Coronary disease, %	13.8	14.3	0.496	5.8	10.2	0.278
Atrial fibrillation, %	14.6	24.8	0.007	15.9	10.2	0.244
SBP, mm Hg	148.5 (25.9)	155.6 (28.1)	0.049	154.5 (30.2)	165.9 (28.7)	0.097
DBP, mm Hg	81.7 (3.9)	82.5 (14.7)	0.708	88.6 (17.8)	87.6 (16.8)	0.745
Temperature, °C	36.3 (0.5)	36.3 (0.5)	0.296	36.3 (0.5)	36. (0.8)	0.867
Bood glucose, mg/dl	132.7 (60.5)	140.2 (60.6)	<0.0001	114.5 (28.5)	134.8 (41.8)	0.007
Leukocytes, $\times 10^3$/ml	8.2 (2.4)	9.0 (2.8)	<0.0001	8.3 (2.3)	9.4 (3.3)	0.072
Platelet number, $\times 10^3$/ml	231.1 (65.8)	255.3 (70.0)	0.045	219.8 (52.7)	246.6 (117.1)	0.525
INR	1.1 (0.3)	1.1 (0.2)	0.003	1.2 (0.5)	1.2 (0.5)	0.270
Fibrinogen, mg/dL	452.9 (103.8)	526.9 (130.7)	<0.0001	453.8 (120.5)	504.6 (113.7)	0.161
hs-CRP, mg/dL	1.6 (2.4)	4.6 (7.9)	<0.0001	3.7 (6.8)	5.7 (8.9)	0.083
NIHSS	3 [1, 5]	11 [6, 17]	<0.0001	3 [2,6]	10 [8,15]	<0.0001
END, %	1.6	24.8	<0.0001			
Infarct Volume, ml	10.4 (16.0)	58.8 (81.1)	<0.0001			
TOAST:			0.006			
-Cardioembolic, %	30.4	45.3				
-Atherothrombotic, %	10.1	8.1				
-Lacunar, %	15.0	5.6				
-Undetermined, %	42.1	39.1				
-Others, %	2.4	1.9				
ICH volume on admission, ml				11.2 (11.4)	27.5 (37.8)	<0.0001
Edema volume, ml				7.5 (12.9)	28.8 (36.0)	<0.0001
Topography:						0.232
-Cerebellar %				4.3	6.8	
-Deep %				65.2	50.8	
-Lobar %				24.6	40.7	
-Brain stem %				4.3	1.7	
-Primary intraventricular, %				1.4	0	
Ventricular extension, %				14.5	40.7	0.001
Etiology:						0.318
-Hypertensive, %				63.8	54.2	
-Anticoagulant, %				13.0	15.3	
-Amyloid, %				2.9	10.2	
-Undetermined, %				19.8	17.0	
Tp53 Arg72Pro polymorphism			<0.0001			<0.0001
-*Arg/Arg* genotype, %	42.1	81.4		18.8	91.5	
-*Arg/Pro* genotype, %	47.4	18.6		71.0	8.5	
-*Pro/Pro* genotype, %	10.5	0		10.2	0	

Patients were admitted at the University Hospital of Santiago de Compostela (Galicia, Spain; cohort 1). Functional outcome was evaluated at 3 mo using the mRS. An mRS score >2 was considered poor prognosis. Data are numbers (%), means (SD), or medians [quartiles]. Data were compared among prognosis groups (goor prognosis vs. poor prognosis) using the χ^2 test (proportions), the Student's *t* test (continuous variables with normal distribution), or the Mann-Whitney test (continuous variables without normal distribution, NIHSS). SBP, systolic blood pressure; DBP, diastolic blood pressure; INR, international normalized ratio; hs-CRP, high sensitivity C-reactive protein. Univariate analysis of variables from cohort 2 (Catalonia, Spain) is shown in Table S2.

Table III. Logistic regression analysis showing independent variables associated with poor functional outcome at 3 mo (mRS > 2) after stroke

Variable	Ischemic stroke			ICH		
	OR	95% CI	P-value	OR	95% CI	P-value
Age	1.05	1.00–1.09	0.013	1.07	0.99–1.15	0.059
Diabetes				0.70	0.10–4.86	0.720
Blood glucose				0.99	0.97–1.01	0.720
ICH volume				0.99	0.95–1.03	0.745
Edema volume				1.02	0.97–1.08	0.334
Ventricular Extension				4.82	0.69–33.5	0.112
NIHSS on admission	1.33	1.20–1.48	<0.0001	1.42	1.16–1.72	<0.0001
Infarct volume	1.01	1.00–1.03	0.035			
END	15.29	2.58–90.62	0.003			
Arg/Arg genotype	3.89	1.63–9.28	0.002	360.7	31.5–4,132.1	<0.0001

Patients were admitted at the University Hospital of Santiago de Compostela (Galicia, Spain; cohort 1). OR and their 95% CI were calculated to demonstrate the independent association between poor prognosis and *Arg/Arg* genotype. Analysis of variables from cohort 2 (Catalonia, Spain) is shown in Table S3.

Next, we analyzed baseline demographic and clinical features of stroke patients by outcome groups. We found that the vast majority of *Arg/Arg* patients (81.4 and 76.5%) had poor functional outcome after ischemic stroke, whereas only a small proportion of *Arg/Pro* (18.6 and 23.5%) and none of the *Pro/Pro* patients showed poor prognosis in the two independent cohorts studied (Table II and Table S2). Furthermore, the *Arg/Arg* genotype was an independent marker of poor functional outcome, as revealed by logistic regression analysis after adjustment for age, National Institutes of Health Stroke Scale (NIHSS) score on admission, infarct volume, and early neurological deterioration (END; Table III and Table S3). Regarding the ICH group, most *Arg/Arg* patients (91.5 and 84.6%) had poor functional outcome, whereas this was minimum (8.5 and 15.4%) in *Arg/Pro* and zero in *Pro/Pro* patients (Table II and Table S2). Moreover, the *Arg/Arg* genotype was found to be a highly independent marker of poor prognosis after adjustment for age, diabetes, blood glucose, ICH volume, perihematoma edema, ventricular extension, and NIHSS upon admission (Table III and Table S3). These results reveal, for the first time, that the *Tp53 Arg72Pro* SNP strongly determines functional outcome after stroke, regardless of whether the origin is ischemic or hemorrhagic.

We next analyzed whether the *Arg72Pro* SNP was associated with secondary variables. END, a common complication associated with poor prognosis after ischemic stroke (Castillo et al., 1997; Kwan and Hand, 2006), was more frequent in *Arg/Arg* (17.4%) than in *Arg/Pro* (2%) or *Pro/Pro* (0%) genotypes ($P < 0.0001$). Moreover, the *Arg/Arg* genotype was found to be an independent marker of END (odds ratio [OR] 7.77 [95% confidence interval (CI) 1.72, 35.01], $P = 0.008$) after adjustment for age, diastolic blood pressure, temperature, glucose levels, fibrinogen, high sensitivity C-reactive protein, and NHISS upon admission. The infarct volume values were also significantly higher in *Arg/Arg* when compared with *Arg/Pro* or *Pro/Pro* genotypes (Fig. 1 C); however, we found no independent association between *Arg/Arg* genotype and infarct volume (B −5.51 [95% CI −16.70, 5.69], $P = 0.384$) after adjustment for age, atrial fibrillation, diagnosis (lacunar versus nonlacunar), leukocyte levels, fibrinogen, high sensitivity C-reactive protein, and NIHSS at admission. Accordingly, we matched all patients for acute infarct volume and we found that the proportion of patients with poor functional outcome was always higher in *Arg/Arg* patients when compared with *Arg/Pro* or *Pro/Pro*, independently on the infarct volume (Table S4).

In the ICH patients, no differences were found in the lesion volume (Fig. 1 D) and perihematoma edema volume (Fig. 1 E) among genotypes, but a five- to sevenfold higher residual cavity volume was found in *Arg/Arg* when compared with *Arg/Pro* or *Pro/Pro* genotypes (Fig. 1 F). Further multiple linear regression analysis confirmed that *Arg/Arg* genotype was an independent marker for residual cavity volume (B 15.40 [95% CI 12.17, 18.62], $P < 0.0001$) after adjustment for a history of diabetes, leukocyte counts, platelet count, hematoma volume, perihematoma edema volume, ventricular extension, and NIHSS upon admission. These data further support the link between *Arg/Arg* genotype with poor prognosis after stroke, with good prognosis being mainly restricted to stroke patients with the *Arg/Pro* or the *Pro/Pro* genotypes.

We next aimed to elucidate whether other naturally occurring *Tp53* genotype would also explain functional prognosis after stroke. We focused on the *Ins16bp* polymorphism (Pietsch et al., 2006), an insertion on *Tp53* intron 3 genotype that, being nearby codon 72 polymorphism in exon 4, might potentially explain the proposed association of this allele with poor prognosis in stroke. However, we found no association between *Ins16bp* genotype and functional prognosis after either ischemic stroke (Fig. 1 G) or ICH (Fig. 1 H), despite showing very similar allelic frequencies to those in the *Arg72Pro* genotypes (Table S1). Such similarities in the allelic frequencies of both polymorphisms confirm earlier studies performed in healthy subjects from European populations (Santos et al., 2006; Costa et al., 2008). Thus, functional prognosis

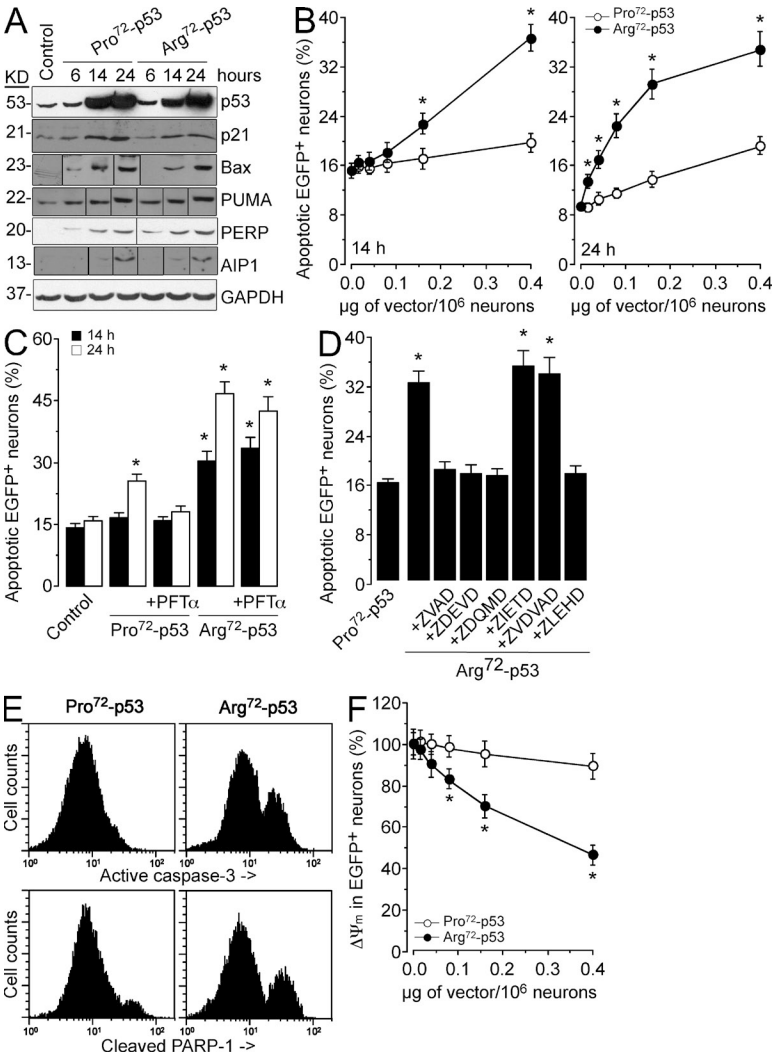

Figure 2. Arg^{72}-p53 triggers neuronal apoptotic death through the intrinsic pathway. (A) HEK293T cells were transfected with empty vector (control) or vector encoding Arg^{72}-p53 or Pro^{72}-p53. At indicated time points, proteins were measured by Western blotting. Black lines indicate that intervening lanes have been spliced out. (B) Rat cortical primary neurons were transfected with vectors encoding Arg^{72}-p53-IRES-EGFP or Pro^{72}-p53-IRES-EGFP. Apoptosis of EGFP$^+$ neurons was measured 14 or 24 h later. (C and D) Neurons transfected as in B were treated with the inhibitor of p53-mediated gene transactivation, PFT-α (C), or with 100 µM of the general caspase inhibitors ZVAD or ZDEVD, 100 µM of the caspase 3 inhibitor ZDQMD, 50 µM of the caspase 9 inhibitor ZLEHD, 100 µM of the caspase 8 inhibitor ZIETD, or 100 µM of the caspase 2 inhibitor ZVDVAD. Apoptosis was measured 14 h later. (E) Neurons transfected as in B were analyzed by flow cytometry. Histograms are gated on EGFP$^+$ cells. (F) $\Delta\psi_m$ was measured in neurons transfected as in B. The data in A and E represent four independent experiments. The data in B–D and F are means ± SEM of four different cell cultures. *, $P < 0.05$ compared with Pro^{72}-p53.

after stroke is strongly associated with *Arg72Pro* SNP and is independent from the potentially nearby linkage disequilibrium associated with the *Ins16bp* polymorphism.

The Arg^{72}-p53 polymorphic variant triggers neuronal death via the mitochondrial apoptotic pathway

Recent studies have shown the occurrence of delayed (days to weeks) apoptotic neuronal death in the surrounding area of the necrotic core, leading to the propagation of brain damage (Broughton et al., 2009). Because the ischemic penumbra (Sairanen et al., 2006) and perihematoma area (Qureshi et al., 2003) show apoptotic neurons that might explain functional outcomes after stroke (Broughton et al., 2009), we next aimed to elucidate whether different *Arg72Pro* genotypes can determine neuronal apoptotic phenotypes. Rat cortical primary neurons (Fig. 2 B and Fig. S1 C) and human neuron-like cells (Fig. S1 D) expressing human Arg^{72}-p53 displayed a clearer apoptotic phenotype than those expressing Pro^{72}-p53, despite the fact that both proteins identically transactivated p53 downstream targets p21 and proapoptotic Bax, PUMA, PERP, and AIP1 (Fig. 2 A). Interestingly, pifithrin α (PFT-α), an inhibitor of p53-mediated transcriptional activation (Zhu et al., 2002; Fig. S1 E), fully prevented the modest Pro^{72}-p53–induced apoptosis without affecting that of Arg^{72}-p53 (Fig. 2 C). It should therefore be noted that in rodents the codon 72 *Tp53* gene exclusively encodes Pro^{72}-p53 (Pietsch et al., 2006), hence explaining why in previous studies PFT-α can improve the recovery of ischemic brain in the rat (Luo et al., 2009). Thus, neuronal apoptotic death by the human-specific Arg^{72}-p53 occurs through a transcriptional-independent mechanism not resembling rodent cell death by p53.

To understand how Arg^{72}-p53 triggered neuronal apoptotic death, we first used a battery of caspase activity inhibitors. We found that, besides the general caspase inhibitors ZVAD and ZDEVD, the highly specific caspase 3 activity inhibitor ZDQMD prevented Arg^{72}-p53–induced neuronal apoptosis (Fig. 2 D). Caspase 3 can be activated by either the mitochondrial-independent caspases 8 and 2 or the mitochondrial-dependent caspase 9; however, inhibition of caspases 8 (ZIETD) or 2 (ZVDVAD) were ineffective, whereas inhibition of caspase 9 with ZLEHD fully prevented Arg^{72}-p53–mediated neuronal apoptosis (Fig. 2 D). Moreover, active caspase 3 and cleaved PARP-1 staining were detected in 30 and 27%, respectively, of enhanced (E) GFP$^+$ neurons efficiently expressing Arg^{72}-p53 but very modestly in those neurons expressing Pro^{72}-p53 (Fig. 2 E). Neurons expressing Pro^{72}-p53 showed intact mitochondrial membrane potential ($\Delta\psi_m$), in contrast to those expressing Arg^{72}-p53 which collapsed their $\Delta\psi_m$ (Fig. 2 F and Fig. S1 F). Together, these results suggest that Arg^{72}-p53 triggers neuronal apoptotic death through the mitochondrial (intrinsic) apoptotic pathway. In good agreement with this notion, we further show that

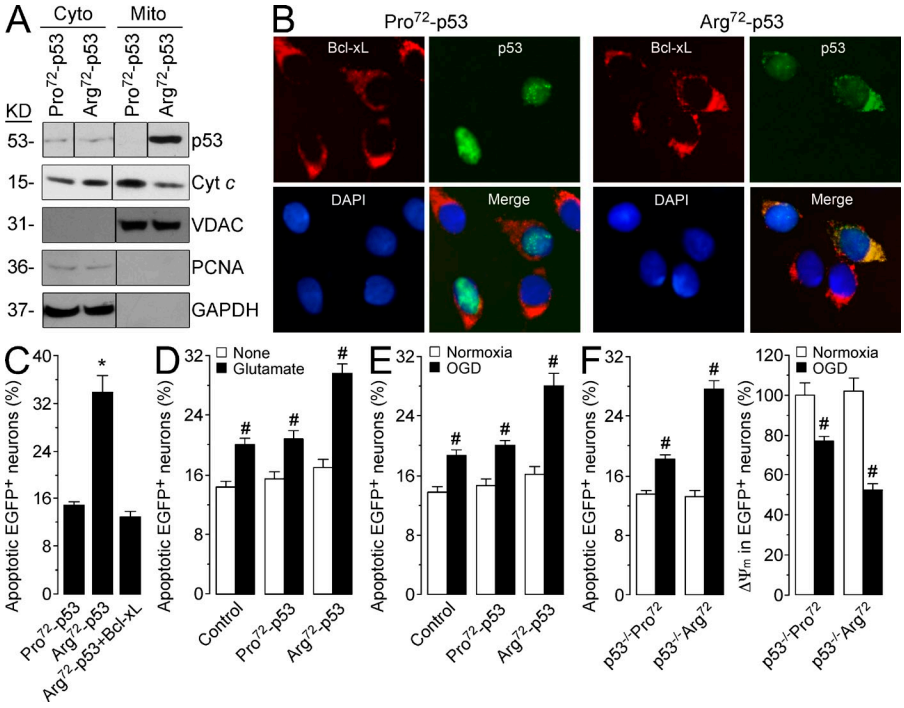

Figure 3. Arg^{72}-p53 interacts directly with mitochondrial Bcl-xL and increases neuronal vulnerability to ischemia-induced apoptosis. (A) HEK293T cells were transfected with Arg^{72}-p53 or Pro^{72}-p53. Cytoplasmic (cyto) and mitochondrial (mito) fractions were isolated and analyzed by Western blotting. VDAC, control for the integrity of the mitochondria. PCNA, control indicating absence of nuclear contamination in the mitochondrial fractions. Black lines indicate that intervening lanes have been spliced out. (B) Rat cortical primary neurons were transfected with Arg^{72}-p53-IRES-EGFP or Pro^{72}-p53-IRES-EGFP. p53 colocalization with Bcl-xL was analyzed by immunofluorescence. DAPI, nuclear staining. (C) Rat cortical primary neurons were transfected with Arg^{72}-p53-IRES-EGFP, Pro^{72}-p53-IRES-EGFP, or Arg^{72}-p53-IRES-EGFP + Bcl-xL. Apoptosis was measured 14 h later. (D) Neurons were transfected with empty vector (control) or the minimum amount of Arg^{72}-p53-IRES-EGFP or Arg^{72}-p53-IRES-EGFP cDNA not altering neuronal survival (0.08 µg/10^6 neurons) and were exposed to 100 µM glutamate for 5 min and incubated in culture medium for a further 8 h. Apoptosis was measured. (E) Neurons were transfected as described in D and were exposed to oxygen and glucose deprivation (OGD) for 1 h. Apoptosis was measured. (F) Neurons from *Tp53*$^{-/-}$ mice were transfected with human BAC containing the entire *Tp53* gene locus encoding either proline (p53$^{-/-}$Pro^{72}) or arginine (p53$^{-/-}$Arg^{72}) and were exposed to oxygen and glucose deprivation (OGD) for 3 h. Apoptosis was measured. The data in A and B represent four independent experiments. The data in C–F are means ± SEM of four different cell cultures. *, P < 0.05 compared with Pro^{72}-p53; #, P < 0.05 compared with none in D or normoxia in E and F. Bar, 20 µM.

Arg^{72}-p53, but not Pro^{72}-p53, is localized in the mitochondria and promotes cytochrome *c* release from the mitochondria to the cytosol (Fig. 3 A). Furthermore, Arg^{72}-p53 interacted directly with Bcl-xL in a much more potent fashion than Pro^{72}-p53 (Fig. 2 B and Fig. S1 G), and Bcl-xL overexpression rescued the neuronal apoptotic death phenotype of Arg^{72}-p53 (Fig. 3 C). Thus, it is conceivable that Arg^{72}-p53 translocates to mitochondria, where it directly binds to (and inactivates) Bcl-xL, thus inducing cytochrome *c* release to promote caspase 9 activation (Taylor et al., 2008).

We finally show that the Arg^{72}-p53, but not the Pro^{72}-p53 variant, when expressed at subtoxic concentrations (Fig. 1 A), increased the vulnerability of neurons to glutamate receptor activation and oxygen/glucose deprivation (Fig. 3, D and E)—two cellular models of ischemic damage (Almeida and Bolaños, 2001; Almeida et al., 2002; Maestre et al., 2008)—through the intrinsic pathway (Fig. S1 H). This was further confirmed by expressing bacterial artificial chromosomes (BACs) containing the endogenous promoter-driven human p53 gene harboring either the Arg^{72} or the Pro^{72} allele in p53-null mice primary neurons. The results show that neurons harboring the Arg^{72} allele (p53$^{-/-}$Arg^{72}) were more vulnerable against OGD-triggered apoptotic death and $\Delta\psi_m$ disruption than those harboring the Pro^{72} one (p53$^{-/-}$Pro^{72}; Fig. 3 F), despite the fact that both polymorphic variants are equally sensitive to OGD-mediated p53 protein accumulation (Fig. S1 I).

In summary, in this paper we show that the *Tp53 Arg/Arg* genotype is a genetic marker of poor functional prognosis after stroke. Interestingly, the *Arg/Arg* genotype is associated with good prognosis in anticancer treatments, and Arg^{72}-p53 protects cells against neoplastic development (Pietsch et al., 2006; Whibley et al., 2009). Thus, proapoptotic Arg^{72}-p53 (Dumont et al., 2003; Bonafé et al., 2004; Zhu et al., 2010; this paper) in *Arg/Arg* subjects dictates both poor and good prognoses in stroke and cancer, respectively. This is in good agreement with the recently highlighted notion that oncogenesis and neuronal death may share common mechanistic foundations (Morris et al., 2010). Furthermore, it would be interesting to know whether the prognostic value of the *Arg/Arg* genotype herein described for stroke outcome are also associated with Alzheimer's or Parkinson's Diseases, two neurodegenerative disorders in which apoptotic neuronal death is an underlying mechanism (Ribe et al., 2008; Levy et al., 2009). If so, our results may have wider pathophysiological implications that now need to be investigated.

MATERIALS AND METHODS

Patient cohorts. An observational prospective study was performed on two independent hospital-based cohorts of patients with ischemic stroke or nontraumatic ICH. Inclusion criteria were patients admitted within the first 12 h after the onset of symptoms, or from the start of sleep in those with symptoms upon awakening, who were previously independent for daily living activities (Table S1). Patients admitted to the University Hospital of Santiago de Compostela (Galicia, Spain) during the years 2006–2008 were enrolled in

the study (cohort 1). Of these, ischemic stroke patients receiving tissue plasminogen activator (tPA) treatment (59 intravenously; 6 intraarterially), those included in clinical trials (33), and those showing severe systemic disease (28) were excluded. Intracerebral hemorrhagic patients with structural brain abnormalities (3 arteriovenous malformations; 13 tumors) and those with severe systemic disease (9) were also excluded. In addition, some patients (24) refused to participate in the study, and 36 were lost during the followup. Two biological samples were not genotyped as a result of poor quantity of DNA. Thus, cohort 1 included 408 patients with ischemic stroke (male, 59.3%; mean age, 72.8 ± 12.1 yr) and 128 with ICH (male, 57.8%; mean age, 71.2 ± 12.3 yr).

The second cohort of patients (cohort 2) was admitted to the University Hospital Germans Trias i Pujol (Catalonia, Spain) during the years 2006–2008. Ischemic stroke patients receiving tPA treatment (182 intravenously; 22 intraarterially), those included in clinical trials (57), and those showing severe systemic disease (12) were excluded. Intracerebral hemorrhagic patients with structural brain abnormalities (2 arteriovenous malformations; 11 tumors) and those included in clinical trials (17) were also excluded. Seven biological samples were not genotyped as a result of poor quantity of DNA. Finally, cohort 2 included 103 patients with ischemic stroke (male, 68.9%; mean age, 67.4 ± 10.1 yr) and 48 with ICH (male, 76.6%; mean age, 67.1 ± 12.7 yr).

In all cases, the protocols were approved by the local Ethics Committee (Santiago de Compostela, Barcelona, and Salamanca) and by the institutional review boards of the University of Santiago de Compostela and the University of Salamanca. All patients or their relatives provided their informed consent before taking part of the studies.

Clinical variables. Patients were admitted to the Acute Stroke Units and treated according to the Guidelines of the Cerebrovascular Disease Study Group of the Spanish Society of Neurology (2004). Medical history, potential vascular risk factors, blood and coagulation tests, 12-lead ECG, chest x-ray, and carotid ultrasonography, were recorded upon admission. Stroke subtypes were classified according to the TOAST criteria (Adams et al., 1993). Stroke severity was assessed by a certified neurologist using the NIHSS upon admission, and after 24 and 48 h. END was diagnosed in patients who worsened ≥4 points (NIHSS score) within the first 48 h (Castillo et al., 1997; Kwan and Hand, 2006). Functional outcome was evaluated at 3 mo using the mRS (Table S5). mRS score >2 was considered poor outcome (Sulter et al., 1999; Banks and Marotta, 2007).

Neuroimaging studies. Ischemic stroke patients were subjected to computed tomography (CT) scans upon admission and at days 4–7. The infarct volume was calculated in the second CT scan using the formula $0.5 \times a \times b \times c$, where a and b represent the largest perpendicular diameters, and c represents the slice thickness. Lesion volumes of the intracerebral hemorrhagic patients were determined by CT scans using the same formula. The hematoma volume was determined upon admission, and the perihematoma edema volume (total volume minus hematoma volume) in a second CT performed after 48–72 h. The residual cavity volume was determined with CT at 3 mo ± 15 d. ICH topography was classified as lobar when it mainly affected the cortical or subcortical white matter of the cerebral lobes or as deep when it was limited to the internal capsule, the basal ganglia, or thalamus. The presence of ventricular extension of the hematoma was also recorded. All neuroimaging evaluations were performed by neuroradiologists blinded to the patients' clinical and laboratory results.

Outcome variables. The main outcome measure for all patients was functional status at 3 mo ± 15 d. In the case of the ischemic stroke patients, secondary variables were infarct volume and END. For ICH, the residual cavity volume was considered to be the secondary variable.

Tp53 polymorphism analysis. Genotyping of *Tp53* polymorphisms was performed at the University of Salamanca, by authors blinded to the clinical status of patients, using the PCR-RFLP technique (Matlashewski et al., 1987; Lazar et al., 1993). The *Tp53* SNP of exon 4 at codon 72 (*Arg72Pro*; rs1042522) was detected by amplifying genomic DNA with the forward primer 5′-TGCCGTTCCCCCTGACATCT-3′ and the reverse primer 5′-CTGACCGTGCAAGTCACAGA-3′. The 16-bp duplication polymorphism at intron 3 (*Ins16bp*; rs17878362) was detected by amplifying genomic DNA with the forward primer 5′-CAGGGAAAAGGGGCACAGAC-3′ and the reverse primer 5′-CCTCCTCCCCACAACAAAACACC-3′. Tp53 exon 4, where BstU1 RFLP is located, was amplified within a 298-bp DNA fragment. The *Tp53 Ins16bp* polymorphism was amplified within a 90-bp (no duplication, designated as the *A1 allele*) or a 106-bp (with 16-bp duplication, designated as the *A2 allele*) DNA fragment. Digests were separated on agarose gel (3.5%) and the ethidium bromide–stained fragments were analyzed under a UV source, using the Kodak Digital Science ID image analysis system. The distribution of genotype frequencies in *Arg72Pro* and *Ins16bp* polymorphisms (Table S1) between the ischemic stroke and the ICH cohorts was within the Hardy-Weinberg equilibrium ($P > 0.1$ in all cases).

Cell cultures, transfections, and treatments. Animals were obtained from the Animal Experimentation Unit of the University of Salamanca, in accordance with Spanish legislation (RD 1201/2005) under license from the Spanish Ministry of Education and Science. Animal experiments were approved by the Bioethics Committee of the University of Salamanca and the Experimental Research Unit of the University Hospital of Salamanca. The mechanistic experiments were performed at the University Hospital of Salamanca. Primary cultures of cortical neurons were prepared from fetal (E16) Wistar rats. Cortical neurons were also obtained from fetal (E15) p53-null mice (*Tp53*$^{-/-}$, The Jackson Laboratory; B6.129S2, donated by I. Garcia-Higuera, Instituto de Biologia Molecular y Celular del Cancer, CSIC-University of Salamanca, Spain). Cells were seeded (2.0×10^5 cells/cm^2) in DME (Sigma-Aldrich) supplemented with 10% (vol/vol) FCS (Roche) and incubated at 37°C in a humidified 5% CO_2-containing atmosphere. 48 h after plating, the medium was replaced with DME supplemented with 5% horse serum (Sigma-Aldrich) and with 20 mM D-glucose. On day 4, cytosine arabinoside (10 µM; Sigma-Aldrich) was added to prevent nonneuronal proliferation (Almeida and Bolaños, 2001). Transfections in primary neurons were performed after 5 d in culture (Almeida et al., 2005). Human neuroblastoma SH-SY5Y cells were grown in DME supplemented with 10% (vol/vol) FCS. To induce neuronal differentiation of SH-SY5Y cells, they were seeded at 10^4 cells/cm^2 and *all-trans* RA (10 µM; Sigma-Aldrich) was added 24 h later. After 5 d, cells were washed three times with DME and further incubated with 50 ng/ml BDNF (PeproTech) for 24 h. Transfections of SH-SY5Y cells were performed after RA for 5 d, i.e., when cells displayed a terminally differentiated neuronal-like phenotype (Almeida et al., 2005). Human embryonic kidney 293T (HEK293T) cells and human p53-null H1299 cells were maintained in DME supplemented with 10% (vol/vol) FCS.

Cells were transfected with the pIRES2-EGFP mammalian expression vector (Invitrogen) coexpressing the EGFP and either the full-length Arg^{72}-p53 or Pro^{72}-p53 human cDNA using Lipofectamine 2000 (Invitrogen; Almeida et al., 2005). Neurons from *Tp53*$^{-/-}$ mice and H1299 cells were transfected with human BACs containing the entire *Tp53* gene locus encoding either arginine (Arg^{72}) or proline (Pro^{72}) at codon 72 (donated by D.G. Johnson, the University of Texas M.D. Anderson Cancer Center, Houston, TX; Zhu et al., 2010) using Lipofectamine 2000. When indicated, cells were treated with 100 µM glutamate for 5 min (Almeida and Bolaños, 2001; Maestre et al., 2008) or exposed to oxygen and glucose deprivation (Almeida et al., 2002).

Flow cytometric analysis of apoptotic cell death. Neurons were stained with APC-conjugated annexin-V and 7-amino-actinomycin D (7-AAD; BD) and were analyzed on a FACSCalibur flow cytometer (BD). EGFP$^+$ (transfected) annexin V–APC-stained cells that were 7-AAD-–negative were considered apoptotic (Almeida et al., 2005; Maestre et al., 2008).

Detection of caspase 3 activation. Active caspase 3 was detected in the transfected (EGFP$^+$) neurons by flow cytometry, using the APO ACTIVE 3 kit (Bachem). Flow cytometric detection of cleaved PARP-1 was performed using the 3-PE anticleaved PARP-1 monoclonal antibody (F21-852; BD).

Flow cytometric analysis of $\Delta\psi_m$. This was assessed in the EGFP$^+$-expressing cells using a MitoProbe DiC1(5) Assay kit for Flow Cytometry (Invitrogen). $\Delta\psi_m$ values were expressed as percentages, and the 10 µM of mitochondrial uncoupler FCCP was used for 15 min to define the 0% $\Delta\psi_m$ values.

Isolation of mitochondria. Mitochondrial fractions were isolated as described in Almeida and Medina (1997), which provides a rapid method for isolation of intact functional mitochondria from cultured cells. In brief, cells were collected in isolation medium (320 mM sucrose, 1 mM potassium EDTA, and 10 mM Tris-HCl, pH 7.4), centrifuged at 600 *g* for 5 min (4°C), and resuspended in isolation medium. Cells were homogenized in a tight-fitting glass-teflon homogenizer (20 strokes) and the nuclei and lysed membranes were removed by centrifugation at 1,500 *g* for 10 min (4°C). We then centrifuged the supernatant at 17,000 *g* for 11 min (4°C) and pellet (mitochondrial fraction) was resuspended in isolation medium. The supernatant contained the cytosolic fraction.

Western blot analysis. Cells were lysed in RIPA buffer (2% sodium dodecylsulphate, 2 mM EDTA, 2 mM EGTA, and 50 mM Tris, pH 7.5), supplemented with phosphatase inhibitors (1 mM Na_3VO_4 and 50 mM NaF) and protease inhibitors (100 µM phenylmethylsulfonyl fluoride, 50 µg/ml antipapain, 50 µg/ml pepstatin, 50 µg/ml amastatin, 50 µg/ml leupeptin, 50 µg/ml bestatin, and 50 µg/ml soybean trypsin inhibitor), and boiled for 5 min. Protein concentrations were determined by the BCA (bicinchoninic acid) method, using bovine serum albumin as a standard (BCA Protein Assay kit; Thermo Fisher Scientific). Aliquots of cell, mitochondrial, or cytosolic extracts were subjected to SDS polyacrylamide gel (Mini-PROTEAN; Bio-Rad Laboratories) and blotted with anti-p53, anti-p21, anticleaved PARP-1 (BD), anti-Bax, anti–active caspase 3 (Santa Cruz Biotechnology, Inc.), anti-PUMA, anti-PERP, anti-AIP1 (Abcam), anti–cytochrome *c* (Santa Cruz Biotechnology, Inc.), anti-VDAC (EMD), anti-PCNA (BD), or anti-GAPDH (Sigma-Aldrich) overnight at 4°C. Signal detection was performed with an enhanced chemiluminescence kit (Thermo Fisher Scientific).

Coimmunoprecipitation assay. Cells were lysed in ice-cold buffer containing 50 mM Tris-HCl, pH 7.5, 150 mM NaCl, 10 mM EDTA, 2 mM EGTA, and 1% NP-40, supplemented with the phosphatase and protease inhibitors cited in Western blot analysis. Cell extracts were clarified by centrifugation and supernatants (500 µg protein) were incubated with 2 µg anti-p53 for 4 h at 4°C, followed by the addition of 30 µl of protein A–Agarose (GE Healthcare) for 2 h at 4°C. Immunoprecipitates were extensively washed with lysis buffer and detected by Western blot analysis (Maestre et al., 2008).

Immunocytochemistry. Neurons grown on glass coverslips were fixed with 4% (vol/vol, in PBS) paraformaldehyde for 30 min and immunostained with rabbit anti–Bcl-xL (1:100) or mouse anti-p53 (1:100; BD) antibodies (Almeida et al., 2005). Immunolabeling was detected using anti–rabbit IgG-Cy3 (1:500) or anti–mouse IgG-Cy5 (1:500; Jackson ImmunoResearch Laboratories, Inc.). Coverslips were washed, mounted in SlowFade light antifade reagent (Invitrogen) on glass slides, and examined using a microscope (Provis AX70; Olympus) equipped with epifluorescence and appropriated filters sets.

Statistical analysis. The results are expressed as percentages for categorical variables. Results from continuous variables are expressed as means (SD) or medians (quartiles), depending on their normal distribution or not. Proportions were compared using the χ^2 test. Student's *t* test or the Mann-Whitney test was used to compare continuous variables between the groups. Spearman analysis was used for bivariate correlations. To exclude a nonrandom mating population, the allele frequencies for Hardy-Weinberg equilibrium were tested with a goodness-of-fit χ^2. The influence of the *Tp53* codon 72 SNP on functional outcome and END was assessed by logistic regression analysis, whereas the influence on volumes was assessed by multiple linear regression models, after adjusting for the main baseline variables related to each main variable in the univariate analysis (enter approach and probability of entry $P < 0.05$). The results are expressed as adjusted ORs with the corresponding 95% CIs. The results obtained in cell cultures are expressed as means ± SEM values from four different culture preparations. In these, statistical analyses were performed by one-way analysis of variance, followed by the least significant difference multiple range test. In these cases, $P < 0.05$ was considered significant. The statistical analyses were conducted using SPSS 16.0 for Macintosh.

Online supplemental material. Fig. S1 shows that Arg72-p53 dictates poor prognosis after both ischemic stroke and intracerebral hemorrhage in the validation cohort and promotes apoptosis through the intrinsic pathway in different cell types. Table S1 shows baseline characteristics of patients. Table S2 includes the univariate analysis of variables according to prognosis in stroke patients from cohort 2 (University Hospital of Germans Trias i Pujol, Catalonia, Spain). Logistic regression analysis showing independent variables associated with poor functional outcome at 3 mo after stroke in cohort 2 is shown in Table S3. Table S4 shows *Tp53 Arg72Pro* genotypes in stroke patients with poor prognosis matched for infarct volume. Table S5 shows mRS. Online supplemental material is available at http://www.jem.org/cgi/content/full/jem.20101523/DC1.

We are especially grateful to Antoni Davalos, Director of the Department of Neurosciences of the Hospital Universitari Germans Trias i Pujol, for his encourage and critical review of the manuscript. We also thank Monica Resch and Monica Carabias for technical assistance.

This work was supported by FEDER (European regional development fund), Instituto de Salud Carlos III (PS09/0366, PI08/1472, and RD06/0026-/0001, -/0013, -/1008), the Junta de Castilla y Leon (GRS244/A/08, GREX206), the Xunta de Galicia (Conselleria de Educacion e Ordenacion Universitaria, 80/2006), Ministerio de Ciencia e Innovacion (SAF2007-66394, SAF2010-20008, and CSD2007-00020), and Caja de Burgos.

The authors have no conflicting financial interests.

Submitted: 28 July 2010
Accepted: 1 February 2011

REFERENCES

Adams, H.P. Jr., B.H. Bendixen, L.J. Kappelle, J. Biller, B.B. Love, D.L. Gordon, and E.E. Marsh III. 1993. Classification of subtype of acute ischemic stroke. Definitions for use in a multicenter clinical trial. TOAST. Trial of Org 10172 in Acute Stroke Treatment. *Stroke*. 24:35–41.

Almeida, A., and J.M. Medina. 1997. Isolation and characterization of tightly coupled mitochondria from neurons and astrocytes in primary culture. *Brain Res.* 764:167–172. doi:10.1016/S0006-8993(97)00453-8

Almeida, A., and J.P. Bolaños. 2001. A transient inhibition of mitochondrial ATP synthesis by nitric oxide synthase activation triggered apoptosis in primary cortical neurons. *J. Neurochem.* 77:676–690. doi:10.1046/j.1471-4159.2001.00276.x

Almeida, A., M. Delgado-Esteban, J.P. Bolaños, and J.M. Medina. 2002. Oxygen and glucose deprivation induces mitochondrial dysfunction and oxidative stress in neurones but not in astrocytes in primary culture. *J. Neurochem.* 81:207–217. doi:10.1046/j.1471-4159.2002.00827.x

Almeida, A., J.P. Bolaños, and S. Moreno. 2005. Cdh1/Hct1-APC is essential for the survival of postmitotic neurons. *J. Neurosci.* 25:8115–8121. doi:10.1523/JNEUROSCI.1143-05.2005

Baird, A.E. 2007. Blood genomics in human stroke. *Stroke*. 38:694–698. doi:10.1161/01.STR.0000250431.99687.7b

Baird, A.E., J. Dambrosia, S. Janket, Q. Eichbaum, C. Chaves, B. Silver, P.A. Barber, M. Parsons, D. Darby, S. Davis, et al. 2001. A three-item scale for the early prediction of stroke recovery. *Lancet*. 357:2095–2099. doi:10.1016/S0140-6736(00)05183-7

Banks, J.L., and C.A. Marotta. 2007. Outcomes validity and reliability of the modified Rankin scale: implications for stroke clinical trials: a literature review and synthesis. *Stroke*. 38:1091–1096. doi:10.1161/01.STR.0000258355.23810.c6

Biros, E., A. Kohút, I. Biros, I. Kalina, E. Bogyiová, and J. Stubna. 2002. A link between the p53 germ line polymorphisms and white blood cells apoptosis in lung cancer patients. *Lung Cancer*. 35:231–235. doi:10.1016/S0169-5002(01)00446-9

Bonafé, M., S. Salvioli, C. Barbi, C. Trapassi, F. Tocco, G. Storci, L. Invidia, I. Vannini, M. Rossi, E. Marzi, et al. 2004. The different apoptotic potential of the p53 codon 72 alleles increases with age and modulates in vivo ischaemia-induced cell death. *Cell Death Differ.* 11:962–973. doi:10.1038/sj.cdd.4401415

Broughton, B.R., D.C. Reutens, and C.G. Sobey. 2009. Apoptotic mechanisms after cerebral ischemia. *Stroke*. 40:e331–e339. doi:10.1161/STROKEAHA.108.531632

Castillo, J. 1999. Deteriorating stroke: diagnostic criteria, predictors, mechanisms and treatment. *Cerebrovasc. Dis.* 9:1–8. doi:10.1159/000047548

Castillo, J., A. Dávalos, and M. Noya. 1997. Progression of ischaemic stroke and excitotoxic aminoacids. *Lancet*. 349:79–83. doi:10.1016/S0140-6736(96)04453-4

Cerebrovascular Disease Study Group of the Spanish Society of Neurology. 2004. Guidelines for the diagnosis and treatment of stroke. Prous Science, Barcelona. 258 pp.

Costa, S., D. Pinto, D. Pereira, H. Rodrigues, J. Cameselle-Teijeiro, R. Medeiros, and F. Schmitt. 2008. Importance of TP53 codon 72 and intron 3 duplication 16bp polymorphisms in prediction of susceptibility on breast cancer. *BMC Cancer*. 8:32. doi:10.1186/1471-2407-8-32

Dumont, P., J.I. Leu, A.C. Della Pietra III, D.L. George, and M. Murphy. 2003. The codon 72 polymorphic variants of p53 have markedly different apoptotic potential. *Nat. Genet.* 33:357–365. doi:10.1038/ng1093

Kwan, J., and P. Hand. 2006. Early neurological deterioration in acute stroke: clinical characteristics and impact on outcome. *QJM*. 99:625–633. doi:10.1093/qjmed/hcl082

Lazar, V., F. Hazard, F. Bertin, N. Janin, D. Bellet, and B. Bressac. 1993. Simple sequence repeat polymorphism within the p53 gene. *Oncogene*. 8:1703–1705.

Levy, O.A., C. Malagelada, and L.A. Greene. 2009. Cell death pathways in Parkinson's disease: proximal triggers, distal effectors, and final steps. *Apoptosis*. 14:478–500. doi:10.1007/s10495-008-0309-3

Luo, Y., C.C. Kuo, H. Shen, J. Chou, N.H. Greig, B.J. Hoffer, and Y. Wang. 2009. Delayed treatment with a p53 inhibitor enhances recovery in stroke brain. *Ann. Neurol.* 65:520–530. doi:10.1002/ana.21592

Maestre, C., M. Delgado-Esteban, J.C. Gomez-Sanchez, J.P. Bolaños, and A. Almeida. 2008. Cdk5 phosphorylates Cdh1 and modulates cyclin B1 stability in excitotoxicity. *EMBO J.* 27:2736–2745. doi:10.1038/emboj.2008.195

Matlashewski, G.J., S. Tuck, D. Pim, P. Lamb, J. Schneider, and L.V. Crawford. 1987. Primary structure polymorphism at amino acid residue 72 of human p53. *Mol. Cell. Biol.* 7:961–963.

Morris, L.G.T., S. Veeriah, and T.A. Chan. 2010. Genetic determinants at the interface of cancer and neurodegenerative disease. *Oncogene*. 29:3453–3464. doi:10.1038/onc.2010.127

Muir, K.W., A. Buchan, R. von Kummer, J. Rother, and J.C. Baron. 2006. Imaging of acute stroke. *Lancet Neurol.* 5:755–768. doi:10.1016/S1474-4422(06)70545-2

Olivier, M., R. Eeles, M. Hollstein, M.A. Khan, C.C. Harris, and P. Hainaut. 2002. The IARC TP53 database: new online mutation analysis and recommendations to users. *Hum. Mutat.* 19:607–614. doi:10.1002/humu.10081

Pietsch, E.C., O. Humbey, and M.E. Murphy. 2006. Polymorphisms in the p53 pathway. *Oncogene*. 25:1602–1611. doi:10.1038/sj.onc.1209367

Qureshi, A.I., M.F. Suri, P.T. Ostrow, S.H. Kim, Z. Ali, A.A. Shatla, L.R. Guterman, and L.N. Hopkins. 2003. Apoptosis as a form of cell death in intracerebral hemorrhage. *Neurosurgery*. 52:1041–1047. doi:10.1227/01.NEU.0000057694.96978.BC

Ribe, E.M., E. Serrano-Saiz, N. Akpan, and C.M. Troy. 2008. Mechanisms of neuronal death in disease: defining the models and the players. *Biochem. J.* 415:165–182. doi:10.1042/BJ20081118

Rosamond, W., K. Flegal, K. Furie, A. Go, K. Greenlund, N. Haase, S.M. Hailpern, M. Ho, V. Howard, B. Kissela, et al; American Heart Association Statistics Committee and Stroke Statistics Subcommittee. 2008. Heart disease and stroke statistics—2008 update: a report from the American Heart Association Statistics Committee and Stroke Statistics Subcommittee. *Circulation*. 117:e25–e146. doi:10.1161/CIRCULATIONAHA.107.187998

Sairanen, T., M.L. Karjalainen-Lindsberg, A. Paetau, P. Ijäs, and P.J. Lindsberg. 2006. Apoptosis dominant in the periinfarct area of human ischaemic stroke—a possible target of antiapoptotic treatments. *Brain*. 129:189–199. doi:10.1093/brain/awh645

Sakamuro, D., P. Sabbatini, E. White, and G.C. Prendergast. 1997. The polyproline region of p53 is required to activate apoptosis but not growth arrest. *Oncogene*. 15:887–898. doi:10.1038/sj.onc.1201263

Santos, A.M., H. Sousa, D. Pinto, C. Portela, D. Pereira, R. Catarino, I. Duarte, C. Lopes, and R. Medeiros. 2006. Linking TP53 codon 72 and P21 nt590 genotypes to the development of cervical and ovarian cancer. *Eur. J. Cancer*. 42:958–963. doi:10.1016/j.ejca.2006.01.015

Sulter, G., C. Steen, and J. De Keyser. 1999. Use of the Barthel index and modified Rankin scale in acute stroke trials. *Stroke*. 30:1538–1541.

Taylor, R.C., S.P. Cullen, and S.J. Martin. 2008. Apoptosis: controlled demolition at the cellular level. *Nat. Rev. Mol. Cell Biol.* 9:231–241. doi:10.1038/nrm2312

Weimar, C., A. Ziegler, I.R. König, and H.C. Diener. 2002. Predicting functional outcome and survival after acute ischemic stroke. *J. Neurol.* 249:888–895. doi:10.1007/s00415-002-0755-8

Whibley, C., P.D. Pharoah, and M. Hollstein. 2009. p53 polymorphisms: cancer implications. *Nat. Rev. Cancer*. 9:95–107. doi:10.1038/nrc2584

Zhu, F., M.E. Dollé, T.R. Berton, R.V. Kuiper, C. Capps, A. Espejo, M.J. McArthur, M.T. Bedford, H. van Steeg, A. de Vries, and D.G. Johnson. 2010. Mouse models for the p53 R72P polymorphism mimic human phenotypes. *Cancer Res.* 70:5851–5859. doi:10.1158/0008-5472.CAN-09-4646

Zhu, X., Q.S. Yu, R.G. Cutler, C.W. Culmsee, H.W. Holloway, D.K. Lahiri, M.P. Mattson, and N.H. Greig. 2002. Novel p53 inactivators with neuroprotective action: syntheses and pharmacological evaluation of 2-imino-2,3,4,5,6,7-hexahydrobenzothiazole and 2-imino-2,3,4,5,6,7-hexahydrobenzoxazole derivatives. *J. Med. Chem.* 45:5090–5097. doi:10.1021/jm020044d